Testing Radiation Models Using Spectral Fluxes and Radiances Measured from Aircraft

P. Partain, S. Miller, R. F. McCoy, G. L. Stephens, R. McCoy, and P. M. Gabriel
Department of Atmospheric Science
Colorado State University
Fort Collins, Colorado

Introduction

One of the purposes of the Atmospheric Radiation Measurement (ARM) Program sponsored by the U.S. Department of Energy (DOE) is to provide data to the scientific community concerning radiative flux profiles of the clear and cloudy atmosphere. As an addition to the arsenal of various tools used to acquire atmospheric radiation data, Colorado State University (CSU) developed the scanning spectral polarimeter (SSP) to make airborne and ground-based measurements of radiant flux and intensity (radiance). These measurements are made at up to 44 wavelengths throughout the visible and near-infrared portions of the electromagnetic spectrum. One of the many applications of SSP data is the comparison of observed and modeled radiance and flux to test both parameterizations used in atmospheric radiative transfer models and the consistency between various sensors measuring similar quantities.

This report covers a range of subjects related to the SSP instrument and sample applications of its data, including comparisons between observed and modeled radiative flux. First, technical details of the SSP instrument and its calibration are discussed. Comparisons are then made with the total direct diffuse radiometer (TDDR), a similar instrument that also measures spectral flux. Finally, comparisons between measured and observed flux will be performed for clear and cloudy conditions, including use of SSP radiance data to perform retrievals of surface and cloud optical properties.

The SSP and Its Calibration

The SSP is modular and composed of three components: the optical assembly, the filter and detector assembly, and the mechanical assembly. The SSP radiometer has six re-configurable optical paths, each with a two-color detector. The instrument uses a circular variable filter having a spectral range from 0.4 microns to 1.1 microns. The bandpass varies for each channel and each wavelength, ranging from 0.012 microns to 0.060 microns. The SSP is capable of measuring four radiance polarizations in addition to unpolarized radiance and spectral flux.

Calibration of the SSP has been carried out at Los Alamos National Laboratory and Sandia National Laboratories (SNL). Although there are many details associated with its calibration, only the most important are discussed here. Radiance channels are calibrated with a 12-in. integrating sphere and the flux channel is calibrated with a 40-in. integrating sphere and a standard lamp. A characteristic of any instrument that measures hemispheric flux is its angular response. The SSP angular response for several wavelengths is presented in Figure 1, where the departure from an ideal cosine response including the frontal transmission lobe for near infrared wavelengths is visible. Angular response is measured from –1° to 4° in 0.25° steps, 5° to 65° in 5° steps, and 65° to 90° in 1° steps. To account for an imperfect cosine response, the calibration at SNL was performed using a 40-in. integrating sphere. The temperature response of the entire instrument is also measured and accounted for during calibration. Calibration error estimates include dark-current noise, lamp uncertainties,

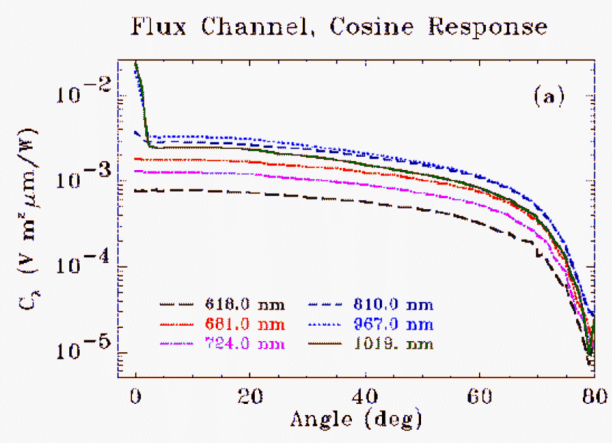

Figure 1. Cosine response of the hemispheric field of view flux wavelengths.

spectral position errors, and temperature errors. Flux and radiance errors are shown in Figures 2 and 3, respectively. Flux errors for most wavelengths are near 5% and radiance errors are around 3% when the temperature of the instrument does not change more than 20°. Error in the raw data arising from aircraft noise can generally be removed with post-processing.

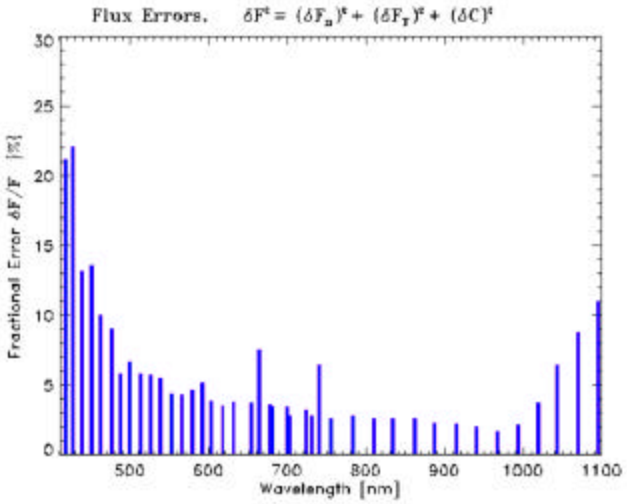

Figure 2. Flux errors as a function of wavelength. (For a color version of this figure, please see *http://www.arm.gov/docs/documents/technical/conf_9803/partain (2)-98.pdf*.)

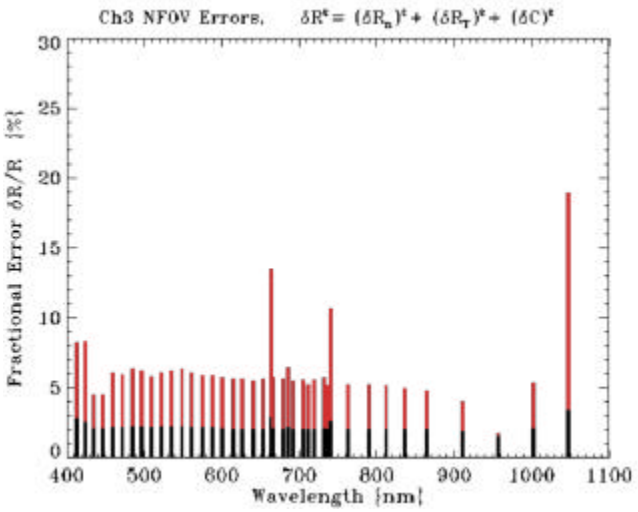

Figure 3. Radiance errors as a function of wavelength. Errors associated with temperature changes smaller than 20° are shown in black. (For a color version of this figure, please see *http://www.arm.gov/docs/documents/technical/conf_9803/partain (2)-98.pdf*.)

Comparisons with instruments that have different optical configurations but measure similar quantities also provide a valuable consistency check. The TDDR is an instrument that also measures spectral flux. Wavelengths common to both the SSP and TDDR include 0.5 microns and 0.862 microns. Scatter plot comparisons between the two instruments at these wavelengths are shown in Figures 4 and 5. Figure 4 presents clear-sky measurements at 0.5 microns

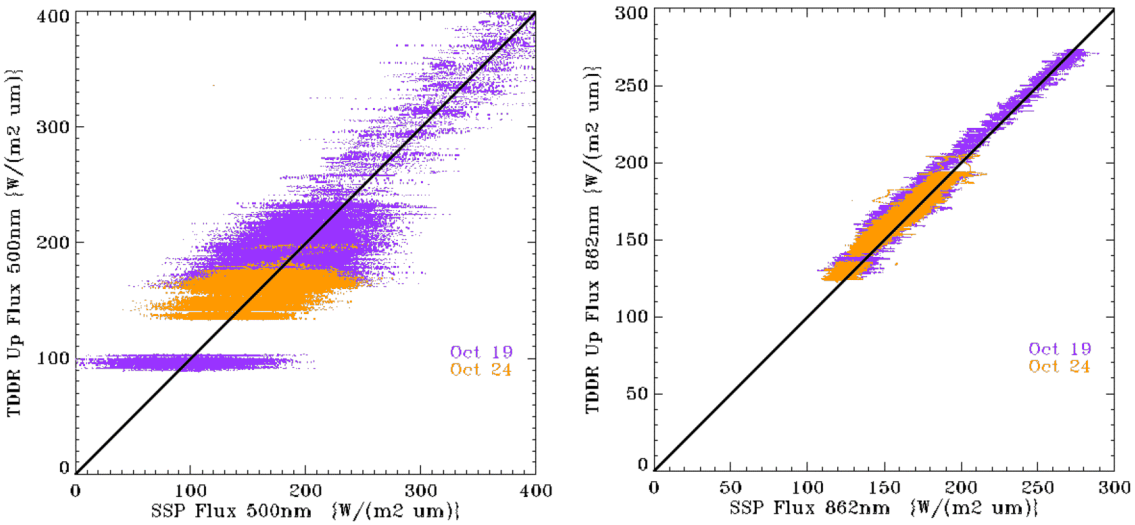

Figure 4. SSP vs. TDDR measurements for clear-sky conditions. (For a color version of this figure, please see *http://www.arm.gov/docs/documents/technical/conf_9803/partain(2)-98.pdf*.)

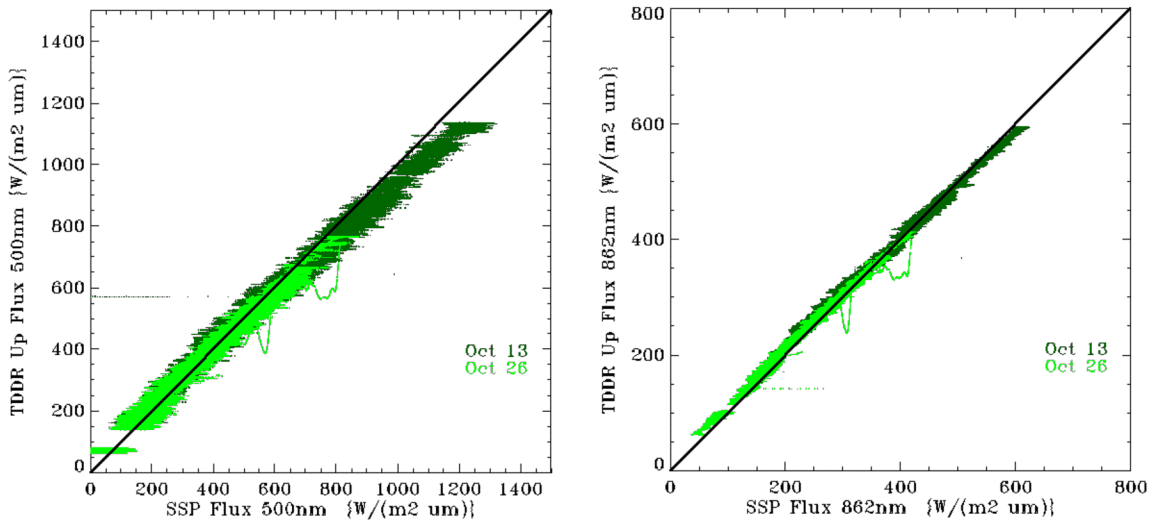

Figure 5. SSP vs. TDDR measurements for cloudy-sky conditions. (For a color version of this figure, please see *http://www.arm.gov/docs/documents/technical/conf_9803/partain(2)-98.pdf*.)

and 0.862 microns. Figure 5 presents cloudy-sky measurements at 0.5 microns and 0.862 microns. Although the SSP data contain more noise, good agreement is achieved.

More details concerning the calibration of the SSP can be found at the SSP homepage at *http://optical.atmos.colostate.edu*.

Applications of the Data

The following sub-sections provide examples of different applications of SSP data. These include retrievals of clear-sky albedo and land-surface albedo (Partain et al. 1998). For this application, the October 11, 1995, case during the ARM Enhanced Shortwave Experiment (ARESE) is analyzed. Another application involves the retrieval of cloud optical properties from SSP spectral radiance and cloud lidar data (Miller et al. 1998) and the subsequent use of these results in two-stream flux calculations to test the consistency between measured radiance, measured fluxes, and model fluxes. Two cloudy-sky cases are analyzed including October 26 and 30 from the ARESE campaign.

Clear-Sky Results

Before a comparison between clear-sky measured and modeled reflected spectral flux at the top of an atmospheric column can be performed, the spectral surface albedo must be retrieved for use as model input. On October 11, 1995, the Egrett aircraft flew three flight legs at low altitude (~2 km) near the Cloud and Radiation Testbed (CART) site. The SSP, which was flown on the aircraft in a nadir-viewing orientation, obtained spectral flux data between 0.4 microns and 1.1 microns. A high spectral resolution two-stream model was run for the time and location of each Egrett flight leg to obtain downwelling flux at the level of the aircraft. The averaged SSP upwelling flux was ratioed with the averaged downwelling flux to obtain a spectral albedo of the surface and atmosphere below the aircraft. The retrieved albedo is plotted in Figure 6. Because this albedo includes atmospheric effects below the aircraft, water vapor spectral

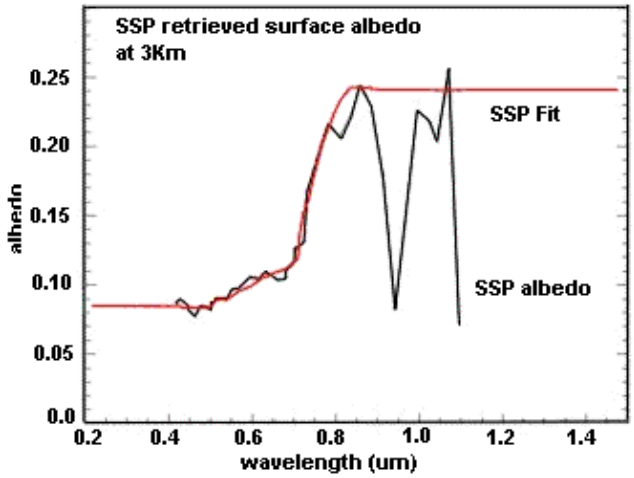

Figure 6. Land surface albedo retrieved by the SSP on October 11, 1995, and curve fit to eliminate water vapor absorption features. (For a color version of this figure, please see *http://www.arm.gov/docs/ documents/technical/conf_9803/partain(2)-98.pdf*.)

absorption lines are observed. To eliminate these absorption features, a smooth fit to the data was made and is also shown in Figure 6. The first and last albedo values were extrapolated to apply to all wavelengths outside of the SSP spectral range. Although the fit eliminates small-scale absorption features, aerosol effects below 2 km are still implicit in the resulting albedo.

This albedo was then used in simulations of reflected and transmitted flux on October 11, 1995. Modeled spectral downwelling and upwelling spectral flux at Egrett altitude (~13 km) and Otter altitude (~2 km) was compared with SSP and TDDR measurements. Because the SSP only flew on the Egrett in a downward looking mode, only modeled upwelling flux at Egrett altitude could be compared with SSP measurements. The results are shown in Figure 7. Model results (solid line) agree well with TDDR measurements (squares). Good agreement is also achieved between model results and SSP measurements (diamonds). However, that agreement deteriorates at shorter wavelengths as model flux exceeds that measured. This is consistent with other findings of enhanced diffuse radiation in clear skies.

Cloudy-Sky Results

Because no in situ measurements of cloud optical properties were made during ARESE, remote retrievals of these properties must be performed to obtain input for the two-stream model. In order to retrieve these properties, SSP radiance data was used in conjunction with lidar cloud height data in an optimal estimation routine following that of Rodgers (1976). This scheme seeks to minimize a cost function that matches forward model radiance with observed radiance given a priori cloud height information and the errors associated with the model, measurements, and a priori information. Output from the retrieval scheme included cloud optical depth, or given the vertical extent of the cloud, cloud extinction (km^{-1}).

The October 26 case consisted of broken cirrus between 8 km and 10 km with some scattered low-level cloud. Figure 8 shows the raw lidar cloud return data (top panel), the retrieved 0.6-micron cloud extinction coefficient (middle panel), and associated optical depth (lower panel) that were used as model input. Because the two-stream model is restricted to plane-parallel, it cannot accommodate cloud heterogeneity that is always observed with real-world cloud structures. In order to compare observed situations that were most similar to model geometry, a simple test was devised to find time periods in the observed data that were most similar to plane-parallel conditions. The test involved the use of the 0.5 micron spectral radiance (I) and flux (F) measured by the SSP. For plane-parallel geometries, the following relationship holds: $F=pI$. If the ratio of pI/F was within 10% of 1.0, the observed scene was marked as "near plane-parallel." Comparisons of modeled and measured 0.5 micron spectral flux is shown in Figure 9 using this simple test. The top panels show the comparison under plane-parallel conditions and a typical cloud scene as photographed from the wide field of view camera flown on the Egrett. The bottom panels show the comparison and a photograph when the above ratio is outside of the 10% limit. In each of the comparison panels, SSP and TDDR data points are plotted. The comparison with model fluxes is good for quasi-plane-parallel conditions, although there is a small bias. Figure 10 presents a comparison of broadband flux between the modeled and data obtained by the Radiation Measurement System (RAMS), also flown on board the Egrett. Again, modeled and measured broadband flux agree well under plane-parallel conditions.

The second cloudy-sky case on October 30 consisted of a stratocumulus cloud located between 1 km and 2 km with some scattered cirrus above. Figure 11 shows the cloud lidar data along with the retrieved cloud extinction coefficient and optical depth. The two-stream model was run with these inputs and comparisons similar to those made for October 26 were performed. Figure 12 shows the scatter plot of 0.5 micron spectral flux using the plane-parallel test. Like the October 26 case, the agreement between the SSP, TDDR, and the model is good aside from a slight bias. Here, there is also a slight difference between the measurements of the SSP and TDDR. When broadband comparisons are performed as in Figure 13, the model reflected flux is much larger than associated measurements. The reason for this difference is not known at this time, although the October 30 case has already been recognized as controversial.

Summary and Conclusions

The SSP provides a valuable dataset to the scientific community for the study of atmospheric radiation. This instrument was designed for deployment on aircraft and at surface sites as part of the ARM Program. Calibration is based on the use of integrating spheres and has been carried out over the past 3 years. Over this time, the SSP has proven to be stable, reliable, and a precise tool for the measurement of atmospheric radiation.

The applications of the data discussed in this report include remote sensing and retrieval of cloud and surface optical properties and comparisons with model-derived radiometric quantities. Other possible applications of SSP data include testing various atmospheric radiative transfer model

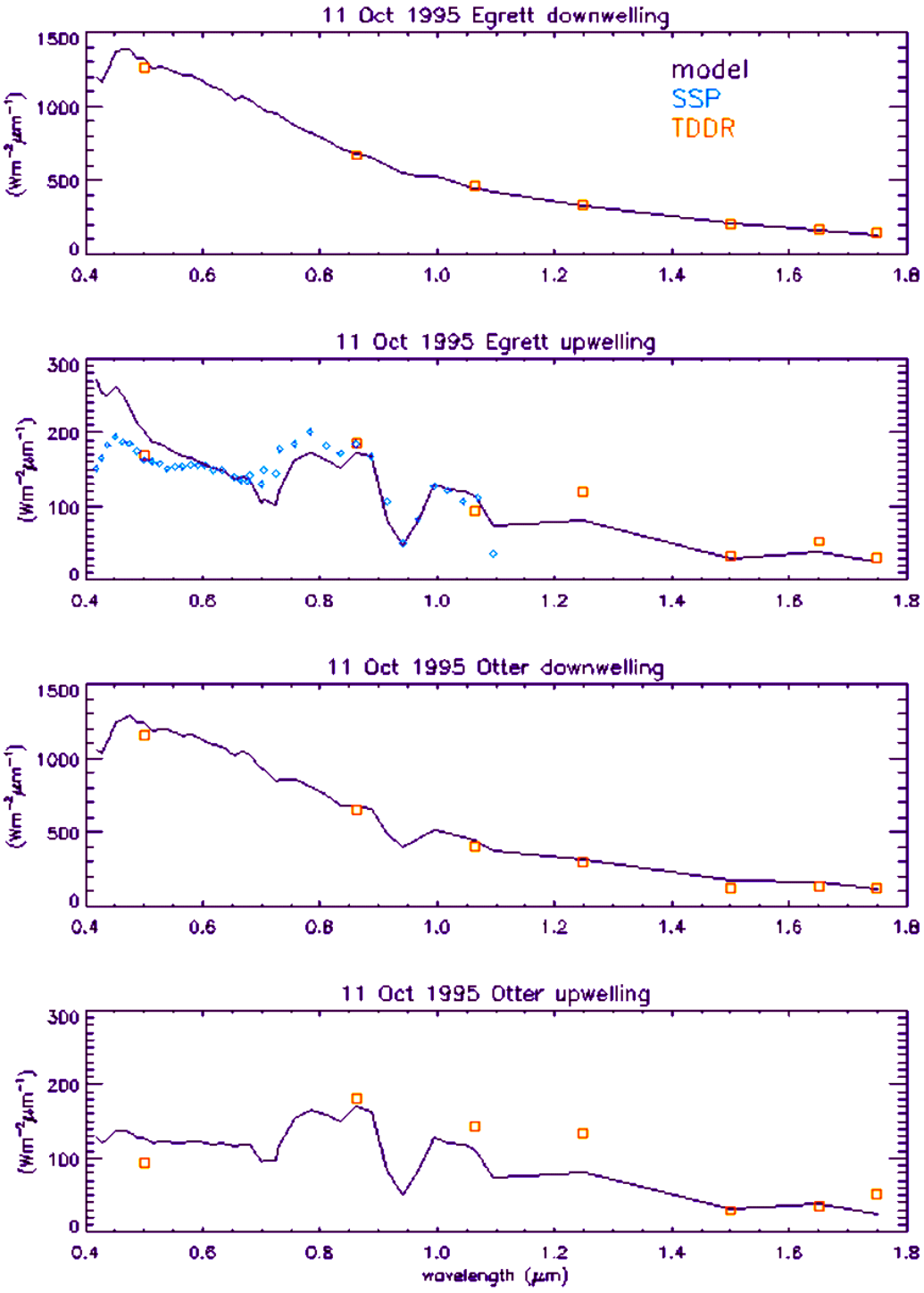

Figure 7. Model simulated spectral flux (solid line), TDDR measurements (squares), and SSP measurements (diamonds) for October 11, 1995. Shown are downwelling and upwelling flux at Egrett and Otter altitude. (For a color version of this figure, please see *http://www.arm.gov/docs/documents/ technical/conf_9803/partain(2)-98.pdf*.)

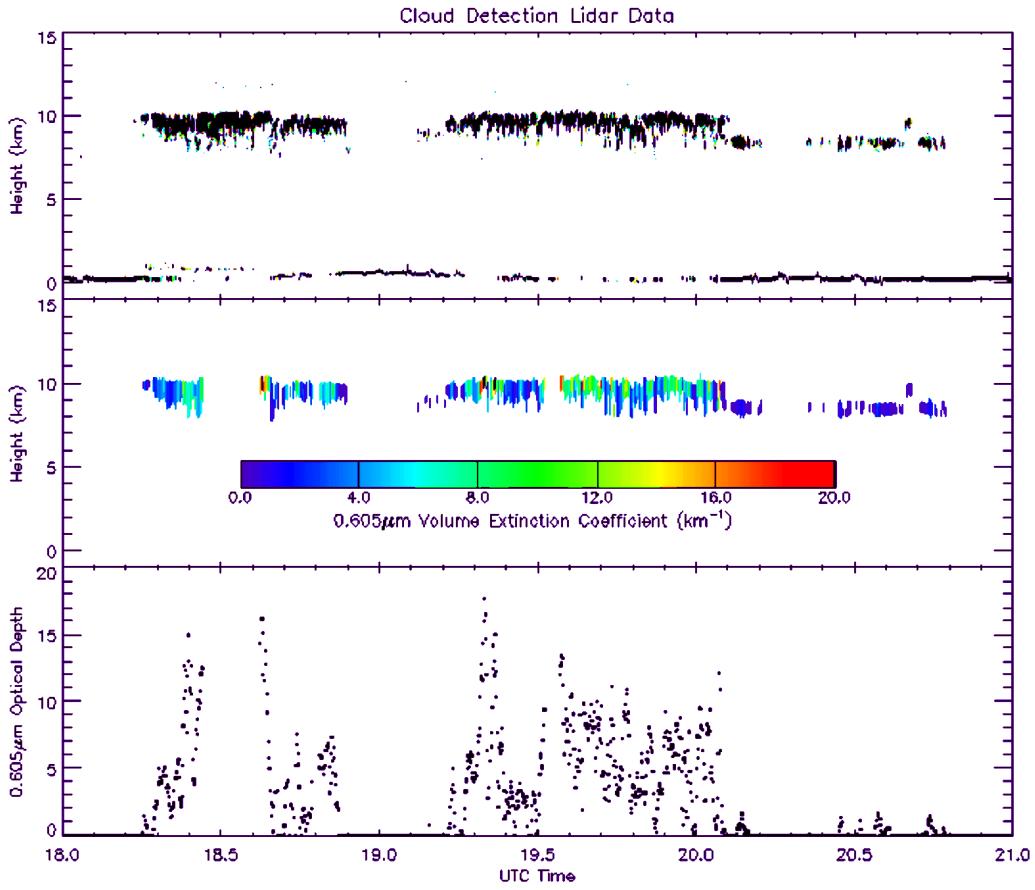

Figure 8. Lidar cloud height data (top), retrieved cloud extinction coefficient (middle), and optical depth (bottom) for October 26, 1995. (For a color version of this figure, please see *http://www.arm.gov/docs/ documents/technical/conf_9803/partain (2)-98.pdf*.)

parameterizations. All of these applications demonstrate the utility of the SSP, especially when used in synergy with other sensors.

Reference

Rodgers, C. D., 1976: Retrieval of atmospheric temperature and composition from remote measurements of thermal radiation. *Reviews of Geophys. and Space Phys.*, **14**, 609-624.

Other Publications in Progress

Miller, S., G. Stephens, C. Drummond, A. Heidinger, and P. Partain, 1998: An active-sensor enhanced multipurpose satellite cloud property retrieval scheme. In preparation.

Partain, P., S. Miller, and G. Stephens, 1998: On the consistency between modeled and measured solar flux reflected by clouds. In preparation.

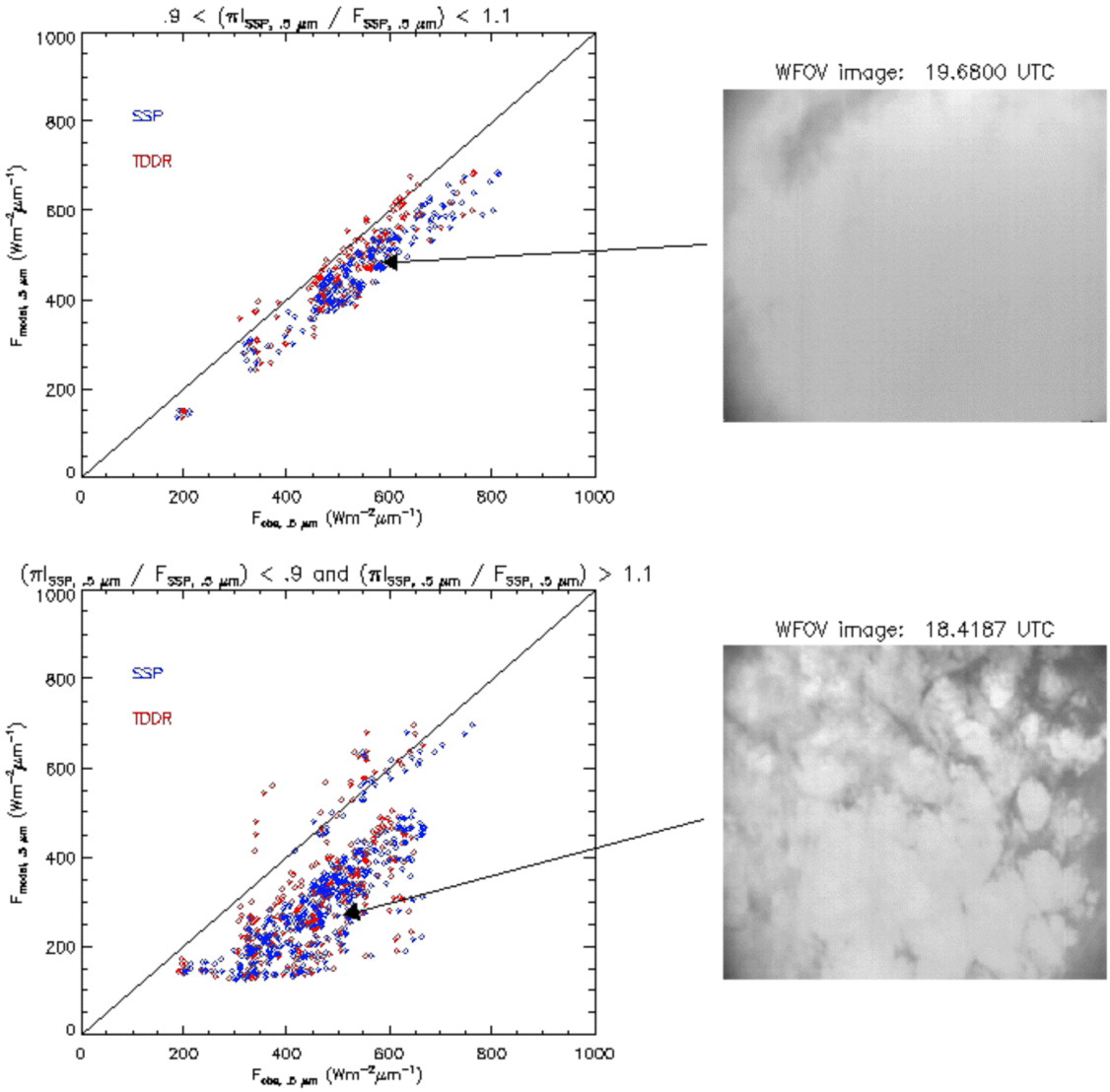

Figure 9. Scatter plots of modeled vs. SSP and TDDR measured upwelling 0.5 micron spectral flux at Egrett altitude for October 26, 1995, using a simple isotropic plane-parallel test. Also shown are typical cloud scenes categorized by the isotropic test. (For a color version of this figure, please see *http://www.arm.gov/docs/ documents/technical/ conf_9803/partain(2)-98.pdf*.)

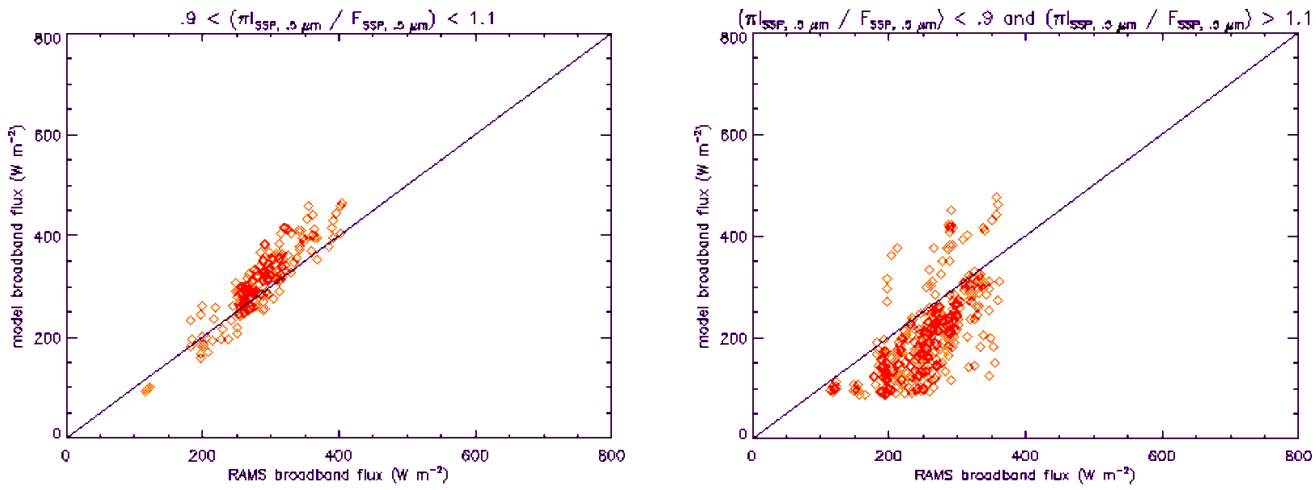

Figure 10. Scatter plots of modeled vs. RAMS measured broadband flux at Egrett altitude for October 26, 1995, using the isotropic test. (For a color version of this figure, please see *http://www.arm.gov/docs/documents/technical/conf_9803/partain(2)-98.pdf*.)

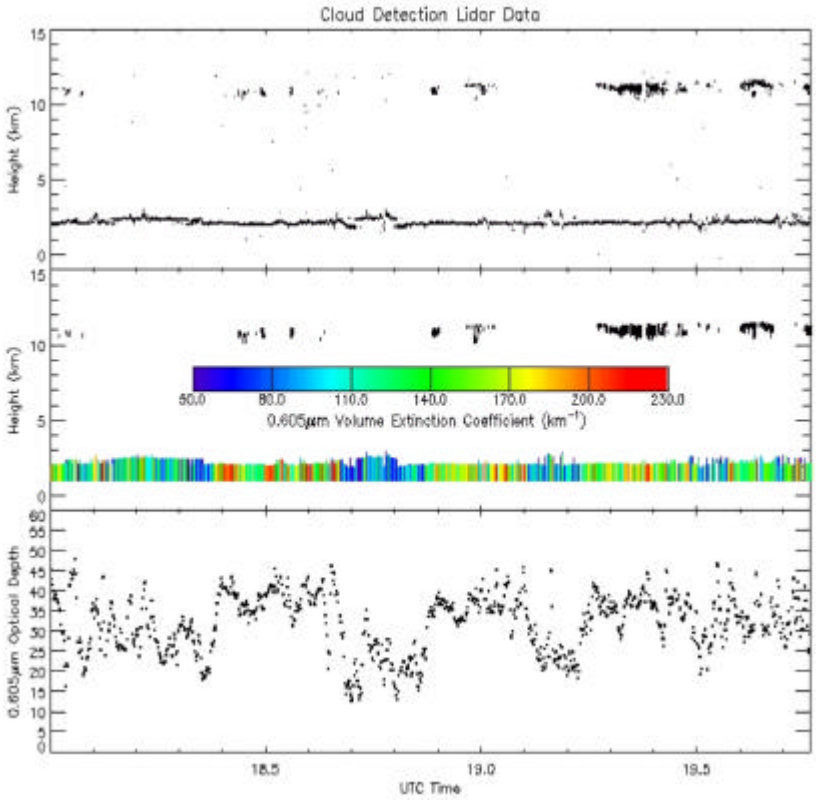

Figure 11. Lidar cloud height data (top), retrieved cloud extinction coefficient (middle), and optical depth (bottom) for October 30, 1995. (For a color version of this figure, please see *http://www.arm.gov/docs/documents/technical/conf_9803/partain(2)-98.pdf*.)

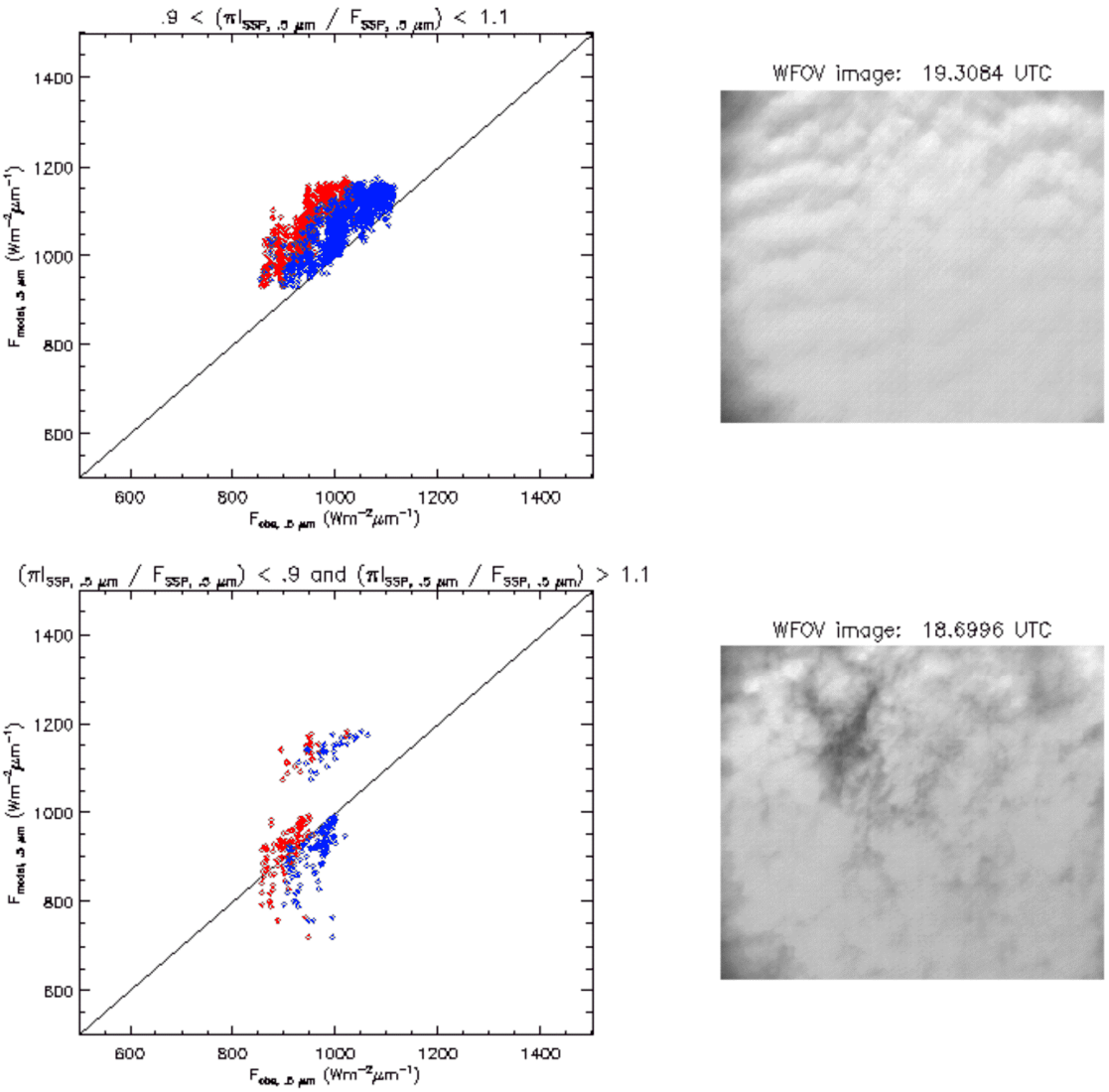

Figure 12. Scatter plots of modeled vs. SSP and TDDR measured upwelling 0.5 micron spectral flux at Egrett altitude for October 30, 1995, using a simple isotropic plane-parallel test. Also shown are typical cloud scenes categorized by the isotropic test. (For a color version of this figure, please see *http://www.arm.gov/docs/documents/technical/conf_9803/partain(2)-98.pdf*.)

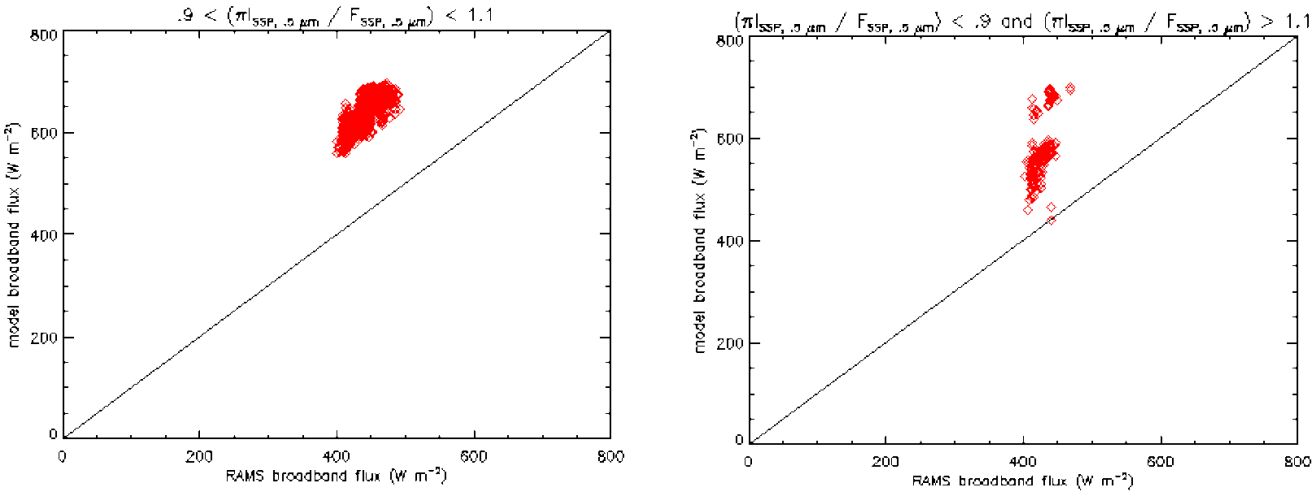

Figure 13. Scatter plots of modeled vs. RAMS measured broadband flux at Egrett altitude for October 30, 1995, using the isotropic test. (For a color version of this figure, please see *http://www.arm.gov/docs/documents/technical/conf_9803/partain(2)-98.pdf*.)